Calcium isotope ($\delta^{44/40}$Ca) variations of Neogene planktonic foraminifera

Alexander Heuser,[1] Anton Eisenhauer,[1] Florian Böhm,[1] Klaus Wallmann,[1]
Nikolaus Gussone,[1,2] Paul N. Pearson,[3] Thomas F. Nägler,[4]
and Wolf-Christian Dullo[1]

[1]   Measurements of the calcium isotopic composition ($\delta^{44/40}$Ca) of planktonic foraminifera from the western equatorial Pacific and the Indian sector of the Southern Ocean show variations of about 0.6‰ over the past 24 Myr. The stacked $\delta^{44/40}$Ca record of *Globigerinoides trilobus* and *Globigerina bulloides* indicates a minimum in $\delta^{44/40}$Ca$_{sw}$ (seawater calcium) at 15 to 16 Ma and a subsequent general increase toward the present, interrupted by a second minimum at 3 to 5 Ma. Applying a coupled calcium/carbon cycle model, we find two scenarios that can explain a large portion of the observed $\delta^{44/40}$Ca$_{sw}$ variations. In both cases, variations in the Ca input flux to the ocean without proportional changes in the carbonate flux are invoked. The first scenario increases the riverine calcium input to the ocean without a proportional increase of the carbonate flux. The second scenario generates an additional calcium flux from the exchange of Ca by Mg during dolomitization. In both cases the calcium flux variations lead to drastic changes in the seawater Ca concentrations on million year timescales. Our $\delta^{44/40}$Ca$_{sw}$ record therefore indicates that the global calcium cycle may be much more dynamic than previously assumed.

Citation: Heuser, A., A. Eisenhauer, F. Böhm, K. Wallmann, N. Gussone, P. N. Pearson, T. F. Nägler, and W.-C. Dullo (2005), Calcium isotope ($\delta^{44/40}$Ca) variations of Neogene planktonic foraminifera, *Paleoceanography*, *20*, PA2013, doi:10.1029/2004PA001048.

1.   Introduction

[2]   Foraminifera are important marine archives. Their oxygen and carbon isotope composition as well as several element/calcium ratios (e.g., Mg/Ca) of their shells are used as proxies for the reconstruction of past climate and environmental conditions [e.g., *Farrell and Prell*, 1991; *Hastings et al.*, 1998; *Lear et al.*, 2000; *Rosenthal et al.*, 1997; *Billups and Schrag*, 2003]. For the reconstruction of past changes of continental erosion and chemical weathering usually strontium (^{87}Sr/^{86}Sr) and neodymium (^{143}Nd/^{144}Nd) isotopes are applied because the different rock end-members are considerably different in their isotopic composition [e.g., *Jacobson et al.*, 2002; *Harris*, 1995; *Vance and Burton*, 1999]. Calcium is a major component of the continental weathering flux. Thus records of the isotopic composition of seawater calcium ($\delta^{44/40}$Ca$_{sw}$) are used to study variations of the weathering flux during the Cenozoic and Cretaceous [*De La Rocha and DePaolo*, 2000; *Schmitt et al.*, 2003a; *Soudry et al.*, 2004].

[3]   Isotope ratios of seawater calcium ($\delta^{44/40}$Ca$_{sw}$) can be reliably recorded in foraminiferal tests [*Gussone et al.*, 2003]. Recent advancements in mass spectrometry [*Heuser et al.*, 2002; *Fietzke et al.*, 2004] allow a faster processing of $\delta^{44/40}$Ca measurements enabling high-resolution investigations of Ca isotope variations in foraminifera and other carbonates. With that, calcium isotope ratios in foraminiferal tests are a new and promising proxy for investigating cation fluxes to and from the oceans.

[4]   While calcium isotope variations in foraminifers reflect variations of $\delta^{44/40}$Ca$_{sw}$, they may also be influenced by seawater temperature [*Nägler et al.*, 2000; *Zhu and Macdougall*, 1998]. In a systematic study on the influence of seawater temperature on the $\delta^{44/40}$Ca ratios of biogenic and inorganic CaCO$_3$, *Gussone et al.* [2003] investigated temperature-dependent calcium isotope fractionation of laboratory cultured *Orbulina universa* and inorganically precipitated aragonite. For both they reported a $\delta^{44/40}$Ca-temperature gradient of 0.019 ± 0.003‰ °C^{-1} and 0.015 ± 0.002‰ °C^{-1}, respectively. For two other foraminiferal species *Nägler et al.* [2000] (*Globigerinoides sacculifer*) and *Hippler et al.* [2002] (*Neogloboquadrina pachyderma* sinistral) found much steeper $\delta^{44/40}$Ca-temperature gradients of about 0.2‰ °C^{-1}. Following a theoretical approach *Gussone et al.* [2003] proposed that the different $\delta^{44/40}$Ca-temperature gradients of *O. universa* and *G. sacculifer* can be explained by different biochemical processes related to their kinetically controlled calcite precipitation mechanisms.

[5]   Here we present the first data of $\delta^{44/40}$Ca variations of three species of planktonic foraminifers (*Globigerionides*

---

[1]Leibniz-Institut für Meereswissenschaften, Kiel, Germany.
[2]Now at Forschungszentrum Ozeanränder, Universität Bremen, Bremen, Germany.
[3]Department of Earth Sciences, Cardiff University, Cardiff, UK.
[4]Institut für Geologie, Gruppe Isotopengeologie, Universität Bern, Bern, Switzerland.
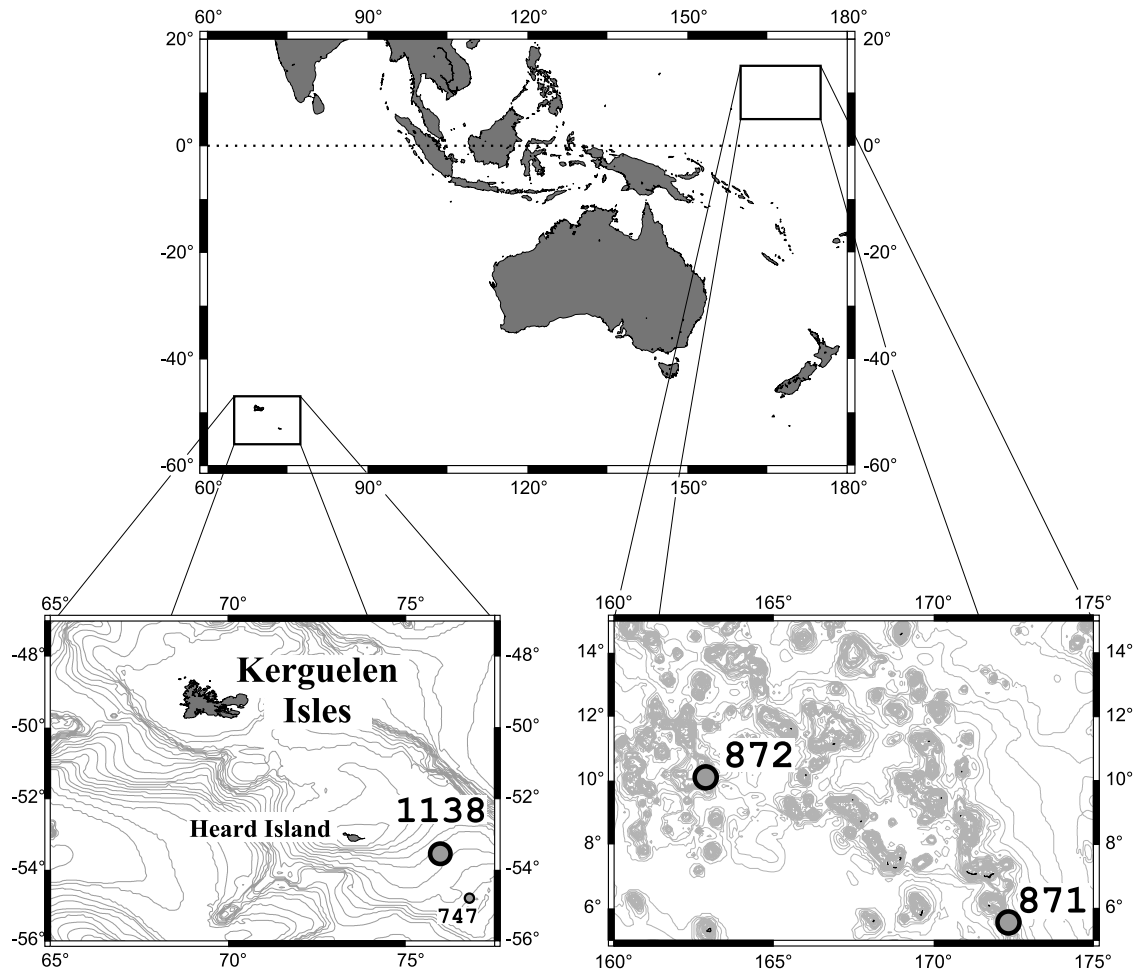
Figure 1. Locations of the Ocean Drilling Program (ODP) Sites 144–871 and 144–872 in the western equatorial Pacific and ODP Site 183–1138 in the southern Indian Ocean.

trilobus, Globigerionides ruber/subquadratus and *Globigerinella* spp.) from the western equatorial Pacific and one species (*Globigerina bulloides) from* the Indian sector of the Southern Ocean over the past 24 Myr. The goal of this study is to apply foraminifers as archives for past $\delta^{44/40}$Ca variations of calcium dissolved in the ocean waters. This study completes and extends earlier studies of *De La Rocha and DePaolo* [2000] and *Schmitt et al.* [2003a] which showed that the $\delta^{44/40}$Ca of seawater varied by up to 0.9‰ during the last 80 million years (Myr).

2. Materials

[6] We investigated planktonic foraminifers (*Globigerinoides trilobus, Globigerinoides ruber, Globigerinella* spp. and *Globigerina bulloides*) from two different regions (Figure 1). The species *G. trilobus, G. ruber* and *Globigerinella* spp. were selected from ODP Leg 144 Sites 871 (Limalok Guyot) and 872 (Lo-En Guyot) in the western equatorial Pacific (871, 5°33.4′N, 172°20.7′E, 1255 mbsl; 872, 10°5.6′N, 162°52.0′E, 1082 mbsl). These sites moved about 7° to the north during the Neogene because of plate tectonic movements. Site 871 crossed the equator around 18 Ma [*Lyle*, 2003]. We use a combined record of Holes

871A and 872C with a temporal resolution of about 1 Ma based on the biostratigraphical and micropaleontological concepts from *Pearson* [1995]. The Leg 144 materials are splits of samples previously used for boron isotope analyses by *Pearson and Palmer* [2000]. Further details on Leg 144 are found in *Premoli Silva et al.* [1993] and *Haggerty et al.* [1995].

[7] *G. bulloides* was sampled from ODP Leg 183 Site 1138 in the southern Indian Ocean (53°33.1′S, 75°58.5′E, 1141 mbsl). Site 1138 is positioned above the Kerguelen hot spot, which has moved less than 10° to the south during the last 100 Myr [*Antretter et al.*, 2002]. Therefore changes in the palaeoposition of Site 1138 during the Neogene are negligible. The analyzed size fraction of *G. bulloides* is 250 to 500 μm. At Site 1138 no samples are available for the time interval from 4.5 to 6.3 Ma (early Pliocene to late Miocene) because of a sedimentary hiatus. The average sample spacing at Hole 1138A corresponds to 1 Ma. Age assignments for Site 1138 are based on our interpretation of combined biostratigraphic and magneto-stratigraphic data [*Coffin et al.*, 2000; *Vigour and Lazarus*, 2002; *Antretter et al.*, 2003; *Bohaty et al.*, 2003]. Details on Leg 183 are given by *Coffin et al.* [2000] and *Frey et al.* [2003].

Table 1. Ca Concentration and Isotope Composition of the Ca Spike

Isotope	^{40}Ca	^{42}Ca	^{43}Ca	^{44}Ca	^{48}Ca
Concentration, ng g^{-1}	8.86	0.46	47.20	2.91	60.00
Isotope ratio	$^{40}Ca/^{48}Ca$	$^{42}Ca/^{48}Ca$	$^{43}Ca/^{48}Ca$	$^{44}Ca/^{48}Ca$	$^{44}Ca/^{40}Ca$
Value	0.147729	0.007668	0.786624	0.048534	0.328537

[8] *G. trilobus* is used as a broad taxonomic concept for *sacculifer*-like specimens that lack a sac shaped final chamber [*Hemleben et al.*, 1989; *Pearson et al.*, 1997]. A classification of these specimens into a number of morphospecies is not applied here. The term *G. ruber* is used as in the work of *Pearson* [1995] and *Pearson and Shackleton* [1995], i.e., including the Miocene species *G. subquadratus* [*Kennett and Srinivasan*, 1983].

[9] The Miocene specimens of *Globigerinella spp.* correspond mostly to *G. praesiphonifera*, which is supposed to be a precursor of modern *G. siphonifera*. In the size fraction used for this study (250 to 300 μm) it is very difficult to distinguish morphospecies like *G. adamsi*, *G. calida* and *G. siphonifera*. Therefore the term *Globigerinella* spp. is commonly used for all these species.

[10] The sediments of the two Pacific sites are characterized by the absence of diagenetic alteration [*Pearson and Palmer*, 2000]. The same applies to Site 1138 which similarly shows a Neogene section preserved as pristine carbonate ooze [*Coffin et al.*, 2000].

3. Methods

3.1. Sample Preparation

[11] The foraminiferal tests were cleaned to remove organics, which can potentially cause isobaric interferences during calcium isotope analyses. About three to six foraminifers (20 to 100 μg) were weighed into a teflon beaker. After adding 100 μL of ultrapure water, the foraminifers were crushed using a small teflon rod. After 2 min of ultrasonic cleaning the water was replaced. This cleaning procedure was repeated six times. During the fourth cleaning step methanol was used instead of water. In the next step, 100 μL of a mixture of 0.1 N NaOH and a drop of 30% H_2O_2 were added to the sample. This solution was heated at about 80°C for 10 min and then ultrasonically cleaned for 2 min. This procedure was repeated twice and followed by three times washing with ultrapure water in an ultrasonic bath for 2 min. Finally the foraminifers were dissolved in 60 μL of ultrapure 2.5 N HCl, evaporated and redissolved in ultrapure 2.5 N HCl with a concentration of 12.5 ng of Ca per μL of sample solution.

3.2. Mass Spectrometry Techniques and Data Reduction

[12] A detailed description of the applied mass spectrometer techniques is given by *Heuser et al.* [2002]. In order to correct for isotope fractionation during measurement procedures we added 60 μL of a $^{43}Ca/^{48}Ca$ double spike solution (Table 1) to 16 μL of the sample solution after the cleaning procedure. The total amount of Ca in the spike/sample mixture was about 200 ng. The spike/sample mixture was evaporated to dryness, redissolved in 1.5 μL ultrapure 2.5 N HCl, and loaded with Ta_2O_5 activator onto

a single zone refined Re filament using a "sandwich technique" similar to [*Birck*, 1986]. The measurements were carried out on a Finnigan MAT 262RPQ+ TIMS at the mass spectrometer facilities of the GEOMAR Research Center for Marine Geosciences in Kiel, Germany (now Leibniz-Institut f. Meereswissenschaften). Samples were heated to a current of 3 A, corresponding to a temperature of about 1500°C with a rate of 240 mA min^{-1}. Further heating was done manually until the intensity on the pilot mass (^{40}Ca) was between 4.5 and 5 V.

[13] For data reduction we use an iterative algorithm based on the routine of *Compston and Oversby* [1969], modified for Ca isotope analysis by replacing the linear fractionation correction term by an exponential term [*Nägler et al.*, 2000; *Heuser et al.*, 2002]. This algorithm calculates the $^{44}Ca/^{40}Ca$ ratio of the sample from the measured $^{44}Ca/^{48}Ca$, $^{43}Ca/^{48}Ca$ and $^{40}Ca/^{48}Ca$ ratios. The data are presented in the common delta notation as $\delta^{44/40}Ca = [(^{44}Ca/^{40}Ca)_{sample}/(^{44}Ca/^{40}Ca)_{standard} - 1]1000$, as suggested by *Hippler et al.* [2003] and *Eisenhauer et al.* [2004].

[14] An in-house CaF_2 standard was used for normalization. Standard measurements were performed at the beginning and end of each day. The mean of these two measurements was used for normalization, except when their $^{44}Ca/^{40}Ca$ difference exceeded the long-term 1σ standard deviation (1σ = 4.78 × 10^{-6}). In this case a drift correction was applied, assuming a linear drift between two measured standards. Following the suggestion of *Coplen et al.* [2002] and *Eisenhauer et al.* [2004] we report $\delta^{44/40}Ca$ values normalized to NIST SRM915a. We renormalized our measurements with the long-term mean $\delta^{44/40}Ca_{SRM915a}$ of our CaF_2 standard of 1.41‰ (n = 109). All $\delta^{44/40}Ca$ values represent the mean of at least two repeated aliquot measurements of an individual sample solution. Statistical uncertainties are given as twice the standard deviation of the mean ($2\sigma_{mean} = 2\sigma/n^{0.5}$).

[15] For the evaluation of the calcium isotope records in the context of global calcium and carbon cycle fluxes we used an expanded version of the numerical model of *Wallmann* [2001]. Details of the model are given in the auxiliary material[1].

4. Results

[16] The results of the Ca isotope measurements are presented in Tables 2 and 3 and shown in Figure 2. All records display $\delta^{44/40}Ca$ variations of 0.5 to 0.6‰ over the past 24 Myr. The three records from the western equatorial

---

[1]Supporting material is available via Web browser or via Anonymous FTP from ftp://ftp.agu.org/apend/" (Username = "anonymous", Password = "guest"); subdirectories in the ftp site are arranged by journal and paper number. Information on searching and submitting electronic supplements is found at http://www.agu.org/pubs/esupp_about.html.
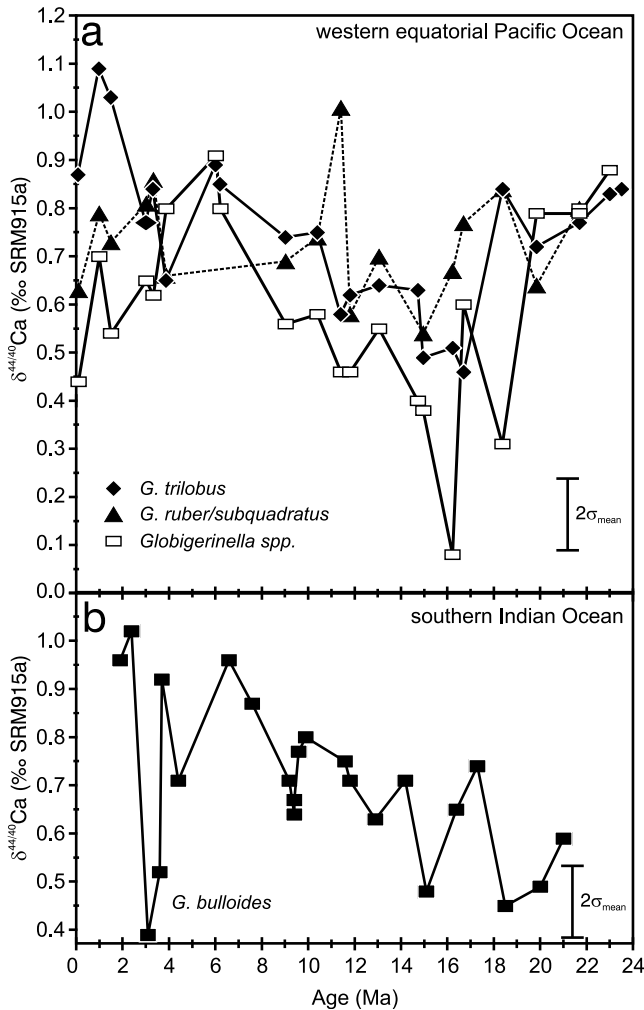
Figure 2. Measured $\delta^{44/40}$Ca values of the foraminifers from the (a) western equatorial Pacific (*G. trilobus, G. ruber/subquadratus,* and *Globigerinella*) and (b) southern Indian Ocean (*G. bulloides*). Error bars represent the average $2\sigma_{mean}$ of all samples.

Pacific Ocean show a decrease in $\delta^{44/40}$Ca from 24 to 16 Ma followed by an increasing trend from about 16 to 15 Ma to the present (Figure 2a). The $\delta^{44/40}$Ca values at the minimum at ~16 Ma differ between species. While it is 0.5‰ for *G. trilobus* and *G. ruber/subquadratus,* it is 0.1‰ in the *Globigerinella* record. During the Miocene (24 to 5 Ma) the $\delta^{44/40}$Ca patterns of the three Pacific species are similar, only the *Globigerinella* values are slightly lighter (~0.2‰) than the $\delta^{44/40}$Ca values of the other two species. In the Pliocene/Pleistocene the $\delta^{44/40}$Ca values of *Globigerinella* spp. are still about 0.2‰ lighter than *G. ruber/subquadratus,* but the $\delta^{44/40}$Ca values of *G. trilobus* are about 0.3‰ heavier than *G. ruber/subquadratus.*

[17] The $\delta^{44/40}$Ca record of *G. bulloides* (Figure 2b) from the southern Indian Ocean shows a minimum of 0.5‰ at about 15 Ma and a subsequent increasing trend to a maximum of about 1.0‰ in the latest Pliocene, similar to the *G. trilobus* record from the western equatorial Pacific. Differing from the Pacific records the 15 Ma minimum is

less pronounced and two additional minima can be seen at about 18 Ma and at 3 Ma.

5. Discussion

[18] In general, $\delta^{44/40}$Ca records of marine shells and minerals primarily reflect variations in the isotopic composition of dissolved seawater calcium (Ca$_{sw}$) [*De La Rocha and DePaolo,* 2000; *Schmitt et al.,* 2003a; *Soudry et al.,* 2004] and of temperature [*Nägler et al.,* 2000; *Gussone et al.,* 2004]. *Gussone et al.* [2003] suggested that foraminiferal species form two distinct groups with different mechanisms of calcification. Ca isotope fractionation in one group is less sensitive to temperature, while in the other group shows a one-order-of-magnitude larger temperature sensitivity. So far, two foraminiferal species belonging to the second group have been identified, *G. sacculifer* and *N. pachyderma.* The temperature-fractionation gradients of these two species have identical slopes but are offset from each other [*Hippler et al.,* 2002]. *Gussone et al.* [2003] explain this different fractionation behavior with different modes of Ca transport at the site of calcification: as hydrated Ca^{2+} ions in the first group or as dehydrated Ca^{2+} ions in the second. The interspecies fractionation offset indicates a biological influence on Ca isotope fractionation in foraminifera of the second group. In group one, on the other hand, the similarity of the gradient to inorganic precipitates and the lack of offsets in the species examined so far indicate a largely abiogenic control of Ca isotope fractionation [*Gussone et al.,* 2003; *Böhm et al.,* 2002, 2003; *Marriott et al.,* 2004; *Lemarchand et al.,* 2004].

[19] Therefore calcium isotope fractionation in foraminifera can be used in a twofold way. Those species showing a weak temperature sensitivity can be used to reconstruct secular variations of $\delta^{44/40}$Ca$_{sw}$. Whereas, those species showing a strong temperature sensitivity are ideally suited to reconstruct paleoseawater temperatures. In the following discussion we first attribute the analyzed species to one of these two groups. We then use the weakly temperature-sensitive species to reconstruct secular variations of $\delta^{44/40}$Ca$_{sw}$ from the Miocene to the present.

5.1. The $\delta^{44/40}$Ca-Temperature Relationship

[20] In order to attribute each analyzed species to one of the two temperature sensitivity groups, we calculate the fractionation factor between seawater calcium and foraminiferal calcite ($\alpha_{cc/sw}$) for the youngest samples of the Pacific cores (0.1 Ma, Table 4), assuming that seawater had the same isotopic composition 0.1 Myr ago as it has today. This assumption is justified by the ocean residence time of calcium of about 0.5 Myr [*Berner and Berner,* 1996]. The fractionation factor $\alpha_{cc/sw}$ is defined as

$$\alpha_{cc/sw} = \left(^{44}Ca/^{40}Ca\right)_{cc} / \left(^{44}Ca/^{40}Ca\right)_{sw}$$
$$= \left(\delta^{44/40}Ca_{cc} + 1000\right) / \left(\delta^{44/40}Ca_{sw} + 1000\right), \quad (1)$$

where cc is calcite and sw is seawater.

[21] We use the $\delta^{44/40}$Ca value of the IAPSO seawater salinity standard as measured at Kiel ($\delta^{44/40}$Ca$_{sw}$ = + 1.82‰

Table 2. Measured $\delta^{44/40}$Ca Values of *G. trilobus*, *G. ruber/subquadratus* and *Globigerinella spp* From ODP Sites 144–871 and 144–872[a]

Hole	Core	Depth, cm	Age, Ma	*G. trilobus* $\delta^{44/40}$Ca	n	*G. ruber* $\delta^{44/40}$Ca	n	Globigerinella $\delta^{44/40}$Ca	n
871A	1H-1	124–126	0.1	0.87 ± 0.05	3	0.63 ± 0.05	2	0.44 ± 0.13	4
871A	2H-2	59–61	1.0	1.09 ± 0.03	2	0.79 ± 0.15	3	0.70 ± 0.23	5
871A	2H-6	59–61	1.5	1.03 ± 0.11	6	0.73 ± 0.19	3	0.54 ± 0.27	5
871A	3H-2	123–125	3.0	0.77 ± 0.13	3	0.81 ± 0.30	6	0.65 ± 0.10	3
872C	3H-2	59–61	3.3	0.84 ± 0.14	5	0.86 ± 0.16	4	0.62 ± 0.21	4
872C	3H-5	118–120	3.9	0.65 ± 0.03	3	0.66 ± 0.19	4	0.80 ± 0.14	4
871A	3H-5	60–62	6.0	0.89 ± 0.10	3	–		0.91 ± 0.13	5
871A	3H-5	123–125	6.2	0.85 ± 0.15	4			0.80 ± 0.25	4
872C	5H-2	14–16	9.0	0.74 ± 0.10	3	0.69 ± 0.09	3	0.56 ± 0.16	4
872C	5H-6	59–61	10.4	0.75 ± 0.10	3	0.74 ± 0.11	3	0.58 ± 0.21	4
872C	6H-5	20–22	11.4	0.58 ± 0.15	4	1.01 ± 0.20	5	0.46 ± 0.20	4
871A	4H-5	59–61	11.8	0.62 ± 0.15	3	0.58 ± 0.08	3	0.46 ± 0.16	4
871A	6H-6	60–62	13.1	0.64 ± 0.16	5	0.70 ± 0.29	5	0.55 ± 0.25	4
871A	7H-2	124–126	14.7	0.63 ± 0.14	6	–		0.40 ± 0.04	3
871A	7H-5	59–61	15.0	0.49 ± 0.15	5	0.54 ± 0.20	5	0.38 ± 0.24	5
871A	8H-2	59–63	16.2	0.51 ± 0.18	6	0.67 ± 0.12	6	0.08 ± 0.06	3
872C	11H-1	20–22	16.7	0.46 ± 0.19	3	0.77 ± 0.21	6	0.60 ± 0.24	3
872C	11H-6	20–22	18.4	0.84 ± 0.07	3	0.84 ± 0.06	2	0.31 ± 0.10	4
872C	12H-2	78–80	19.9	0.72 ± 0.18	2	0.64 ± 0.03	3	0.79 ± 0.10	2
872C	13H-3	20–22	21.7	0.77 ± 0.09	3	0.80 ± 0.20	4	0.79 ± 0.25	3
872C	13H-5	20–22	23.0	0.83 ± 0.22	3	–		0.88 ± 0.29	3
872C	14H-4	20–22	23.5	0.84 ± 0.17	6	–		–	

[a]Values are given as ‰ SRM915a, the National Institute of Standards and Technology standard.

[*Hippler et al.*, 2003]) to represent modern seawater. Concerning Core 1138A, we cannot calculate $\alpha_{cc/sw}$ for the youngest sample of *G. bulloides* from modern seawater because this sample is significantly older (1.9 Ma) than the residence time of Ca in the oceans. The $\delta^{44/40}$Ca$_{sw}$ at 1.9 Ma may have differed significantly from the modern value. Instead we estimate the $\delta^{44/40}$Ca$_{sw}$ from the *G. trilobus* record at 1.5 Ma ($\delta^{44/40}$Ca$_{sw}$ = +1.97‰), assuming negligible temperature variations at that site in the time interval

Table 3. Measured $\delta^{44/40}$Ca Values of *G. bulloides* From ODP Site 183–1138

Sample	Core	Depth, m below seafloor	Age, Ma	$\delta^{44/40}$Ca, ‰ SRM 915a	n
3327	7R-2	57.67	1.9	0.96 ± 0.04	3
3330	8R-3	67.92	2.4	1.02 ± 0.05	4
3360	9R-2	76.00	3.1	0.39 ± 0.11	3
3392	10R-3	87.00	3.6	0.52 ± 0.09	2
3444	11R-1	93.34	3.7	0.92 ± 0.07	4
3491	12R-2	104.10	4.4	0.71 ± 0.13	3
3564	13R-1	112.94	6.6	0.96 ± 0.13	5
3574	13R-4	117.38	7.6	0.87 ± 0.15	6
3619	14R-2	123.78	9.2	0.71 ± 0.11	2
3660	15R-2	133.00	9.4	0.64 ± 0.06	3
3664	15R-2	134.00	9.4	0.67 ± 0.06	3
3691	16R-3	144.60	9.6	0.77 ± 0.18	4
3769	17R-5	157.12	9.9	0.80 ± 0.04	2
3876	19R-1	169.80	11.6	0.75 ± 0.13	6
3879	19R-4	174.30	11.8	0.71 ± 0.08	4
3923	20R-2	180.98	12.9	0.63 ± 0.12	4
3949	21R-2	190.59	14.2	0.71 ± 0.18	3
3971	22R-1	199.50	15.1	0.48 ± 0.06	4
3990	23R-1	209.11	16.4	0.65 ± 0.08	3
4011	24R-1	217.90	17.3	0.74 ± 0.16	2
4029	25R-1	227.50	18.5	0.45 ± 0.14	4
4094	26R-1	237.12	20.0	0.49 ± 0.13	4
4085	27R-2	248.22	21.0	0.59 ± 0.11	3

from 1.5 to 0.1 Ma and a homogeneous distribution of $\delta^{44/40}$Ca$_{sw}$ in the oceans [*Schmitt et al.*, 2001]. The calculated $\alpha_{cc/sw}$ values are shown in Figure 3 as a function of modern seawater temperature at the sampling sites [*Levitus and Boyer*, 1994] and compared to fractionation factors of cultured foraminifera [*Gussone et al.*, 2003]. Note that the errors introduced by applying modern temperatures to 0.1 Ma samples are most likely negligible for our interpretation. In the western equatorial Pacific sea surface temperatures at 0.1 Ma were only about 1° to 2°C cooler than at present [*Lea et al.*, 2000]. Modern temperatures at the Southern Indian Ocean site are close to freezing and likely were in a similar range since the late Pliocene [*Whitehead and McMinn*, 2002].

[22] The $\alpha_{cc/sw}$ values of *G. ruber/subquadratus* and *Globigerinella spp.* plot on the steep fractionation line of *G. sacculifer*, indicating either a strongly temperature-dependent fractionation or species specific fractionation offsets (Figure 3). Both interpretations indicate that these species may not reliably record $\delta^{44/40}$Ca$_{sw}$.

[23] It is not possible to make an unequivocal inference concerning the $\delta^{44/40}$Ca/temperature relationship for *G. trilobus* from Figure 3 because the α value lies close to the intersection of the two fractionation lines. Nevertheless, within errors the α value of *G. trilobus* is compatible with the weak $\delta^{44/40}$Ca-temperature gradient of *O. universa*. The *G. trilobus* record therefore may be used to reconstruct $\delta^{44/}$

Table 4. Calculated α Values of the Most Recent Foraminifers

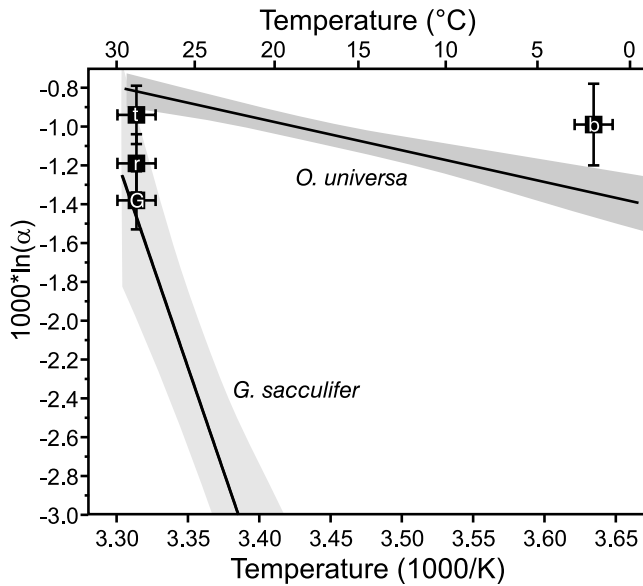|	Age, Ma	$\alpha_{cc/sw}$	1000ln($\alpha_{cc/sw}$)
G. trilobus	0.085	0.99906	−0.94
G. ruber/subquadratus	0.085	0.99881	−1.19
Globigerinella spp.	0.085	0.99862	−1.38
G. bulloides	1.5	0.99901	−0.99

Figure 3. Fractionation factors of *G. ruber/subquadratus* (r), *G. trilobus* (t), *Globigerinella* (G), and *G. bulloides* (b) plotted versus modern water temperatures of the respective foraminiferal habitat (western equatorial Pacific, 28.6°C; southern Indian Ocean, 2°C [*Levitus and Boyer*, 1994]). The fractionation-temperature relationships of *G. sacculifer* [*Nägler et al.*, 2000] and *O. universa* [*Gussone et al.*, 2003] are shown as shaded bars. The *Globigerinella spp.* and *G. ruber/subquadratus* data plot within the *G. sacculifer* trend. The *G. trilobus* value lies near to the intersection of the *O. universa* and *G. sacculifer* trend lines. *G. bulloides* plots close to the *O. universa* trend line.

$^{40}Ca_{sw}$, provided that additional evidence is used to exclude a significant temperature influence. We consequently use this record only in comparison with the record of *G. bulloides*.

[24] Ca isotope data of *G. bulloides* from sediment traps show no significant temperature dependence in a range from 18° to 32°C [*Paytan et al.*, 2004]. We therefore assume a weak temperature dependence for this species, similar to the Ca isotope fractionation trend of *O. universa*. This is further supported by a comparison of the $\delta^{44/40}Ca$ values from Site 1138 with a Mg/Ca record of benthic foraminifers from Site 747, located 150 km southeast of Site 1138 [*Billups and Schrag*, 2003] (Figure 4). This Mg/Ca record indicates a warm period between 20 and 14 Ma followed by a cooling trend from 14 to about 10 Ma (the mid-Miocene climatic optimum and subsequent cooling event [*Flower and Kennett*, 1994]). This mid-Miocene cooling is also well visible in a Southern Ocean sea surface temperature reconstruction from the Tasman Rise [*Shevenell et al.*, 2004], which occupied a similar latitudinal position as Site 1138 during the Miocene. In contrast, the $\delta^{44/40}Ca$ data, if interpreted as a temperature signal, would indicate a cooling between 18 and 15 Ma followed by a warming trend from 15 to about 4 Ma. The strong Pliocene cooling (5 to 2 Ma) of the Mg/Ca record is also not represented in the $\delta^{44/40}Ca$ record of *G. bulloides*, which shows only a short negative

excursion at 3 Ma. These contradictory observations support the inference that the $\delta^{44/40}Ca$ record of *G. bulloides* is not significantly influenced by water temperature.

[25] While the $\delta^{44/40}Ca$ records of all investigated species show the same general trends (Figure 2), we use only the records of *G. bulloides* and *G. trilobus* to reconstruct the Neogene $\delta^{44/40}Ca_{sw}$ history. The *G. ruber/subquadratus* and *Globigerinella spp.* records probably include a temperature signal. This is indicated by their declining trends during the last 3 Myr that we interpret as an indicator of SST cooling in the equatorial Pacific. For our $\delta^{44/40}Ca_{sw}$ reconstruction we use a spline-smoothed stack of the Southern Ocean *G. bulloides* and Pacific *G. trilobus* records. With that we minimize the influence of local factors on our globally representative $\delta^{44/40}Ca_{sw}$ history.

5.2. Reconstruction of Marine Ca Isotope Variations During the Neogene

[26] The $\delta^{44/40}Ca_{sw}$ of dissolved calcium in seawater can be reconstructed from the $\delta^{44/40}Ca$ values of foraminiferal calcite ($\delta^{44/40}Ca_{cc}$) if the corresponding fractionation factor is known (equation 1). We calculated the $\delta^{44/40}Ca_{sw}$ values from the samples of *G. trilobus* and *G. bulloides* using the $\alpha_{cc/sw}$ values calculated from the most recent samples (Table 4) and assuming that the specific fractionation factor was constant throughout time and that temperature effects are negligible for these two species. The two resulting $\delta^{44/40}Ca_{sw}$ records (Table 5) show a good agreement and are in good general agreement with the $\delta^{44/40}Ca_{sw}$ data previously
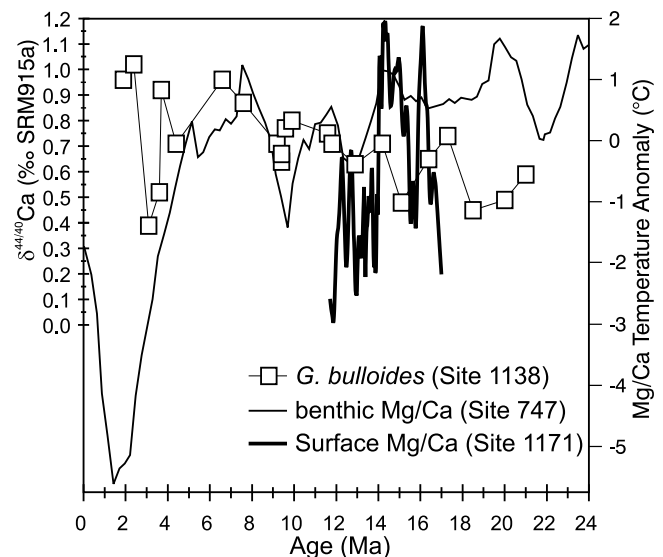

Figure 4. Measured $\delta^{44/40}Ca$ of *G. bulloides* (Site 1138) compared to Mg/Ca-derived temperatures of benthic foraminifera (*Cibicidoides spp.*) from Site 747 [*Billups and Schrag*, 2003] and of *G. bulloides* from Site 1171 [*Shevenell et al.*, 2004]. The $\delta^{44/40}Ca$ axis (left) has been scaled proportional to temperature using the strong temperature dependence from *Nägler et al.* [2000] (1‰ = 4.1°C). Neither the early Miocene warming (24−16 Ma) nor the middle Miocene cooling (15−12 Ma) is reflected in the calcium isotope record.

Table 5. Calculated $\delta^{44/40}Ca_{sw}$

G. trilobus		G. bulloides	
Age, Ma	$\delta^{44/40}Ca_{sw}$	Age, Ma	$\delta^{44/40}Ca_{sw}$
0.1	1.82	1.9	1.95
0.1	2.03	2.4	2.01
1.5	1.97	3.1	1.38
3.0	1.71	3.6	1.51
3.3	1.79	3.7	1.91
3.9	1.60	4.4	1.70
6.0	1.83	6.6	1.95
6.2	1.80	7.6	1.86
9.0	1.69	9.2	1.70
10.4	1.69	9.4	1.63
11.4	1.52	9.4	1.66
11.8	1.56	9.6	1.76
13.1	1.59	9.9	1.79
14.7	1.58	11.6	1.74
15.0	1.43	11.8	1.70
16.2	1.45	12.9	1.62
16.7	1.41	14.2	1.70
18.4	1.78	15.1	1.47
19.9	1.66	16.4	1.64
21.7	1.72	17.3	1.73
23.0	1.78	18.5	1.44
23.5	1.79	20.0	1.48
		21.0	1.58

reported by *De La Rocha and DePaolo* [2000], derived from measurements of marine bulk carbonate sediments (Figure 5). The most significant feature reproduced in all three records is the long-term increase of $\delta^{44/40}Ca_{sw}$ from the early middle Miocene (circa 15 Ma) to the present on the order of about 0.3‰. This overall increase is interrupted by a drop in $\delta^{44/40}Ca_{sw}$ during the Pliocene (3–4 Ma) in both of our records (Figure 6). Latter minimum cannot be seen in the *De La Rocha and DePaolo* [2000] curve because the temporal resolution is too coarse to resolve it.

[27] The early Miocene $\delta^{44/40}Ca_{sw}$ maximum (about 20 to 22 Ma) found by *De La Rocha and DePaolo* [2000] and reproduced by *Schmitt et al.* [2003a] is not well represented in our records. On the other hand, *Schmitt et al.* [2003a], who used Neogene phosphates for their measurements, found no indication of the post-late Miocene increasing trend in their data. We currently have no simple explanation for these discrepancies. *De La Rocha and DePaolo* [2000] used bulk sediment samples for their analyses and do not provide any information about composition, preservation, stratigraphy or sampling locations. It is quite possible that other factors than $\delta^{44/40}Ca_{sw}$, e.g., variations in the sample composition or in water temperatures, were responsible for some of the $\delta^{44/40}Ca$ variations in their record, as is indicated by the 0.5‰ range of three contemporary 80 Ma samples. The phosphatic peloids used by *Schmitt et al.* [2003a] form during early diagenesis within the sediment and may derive variable amounts of Ca from the dissolution of carbonate grains. This Ca is depleted in ^{44}Ca by 0.8 to 1.8‰ compared to $\delta^{44/40}Ca_{sw}$ [*Gussone et al.*, 2003]. Thus variable mixtures of seawater and dissolution Ca in sediment pore fluids can potentially cause a $\delta^{44/40}Ca$ range of up to 1.8‰ in early diagenetic phosphates. We therefore suggest that the Neogene $\delta^{44/40}Ca_{sw}$ history is most reliably represented in our stacked $\delta^{44/40}Ca$ record (Figure 6), which is based on two well-dated independent single species

records of well-preserved planktic foraminifera and has a higher age resolution than previous reconstructions.

6. Causes and Implications of the $\delta^{44/40}Ca$ Variations in Seawater

6.1. Global Cycle of Calcium and Its Isotopes

[28] The reconstructed $\delta^{44/40}Ca_{sw}$ record (Figure 6) shows an increasing trend from about 1.6‰ at the beginning of the middle Miocene (15–16 Ma) to about 1.9‰ in the Pleistocene superimposed by short excursions of $\delta^{44/40}Ca$ on the order of about 0.2‰. In this section we discuss possible causes and implications of the observed variations of $\delta^{44/40}Ca_{sw}$.

[29] Concentration and isotopic composition of calcium in seawater are controlled by riverine and hydrothermal inputs as well as by the removal of Ca via carbonate sedimentation and alteration of oceanic crust. The isotopic composition of river water is remarkably homogenous (0.8 ± 0.2‰) and shows no clear relation to lithology and climatic conditions prevailing in the watershed [*Schmitt et al.*, 2003b]. Hydrothermal solutions are not significantly different from river water in their isotopic composition (0.9 ± 0.2‰ [*Schmitt et al.*, 2003b]). Marine carbonate sediments are also rather homogenous (0.9 ± 0.3‰ [*Skulan et al.*, 1997; *Zhu and Macdougall*, 1998; *De La Rocha and De Paolo*, 2000; *Gussone et al.*, 2003; *Böhm et al.*, 2003; N. Gussone et al., Calcium isotope fractionation in calcite and aragonite, submitted to *Geochimica Cosmochimica Acta*, 2005], even though inorganically precipitated aragonite is isotopically depleted with respect to biogenic calcite [*Gussone et al.*, 2003; *Böhm et al.*, 2002]. The $\delta^{44/40}Ca$ values of marine carbonates are positively correlated to temperature so that the isotopic fractionation between
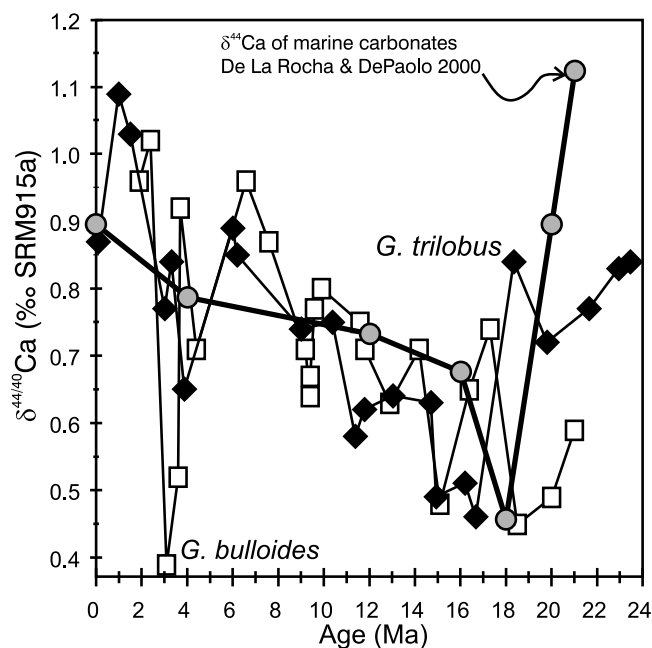

Figure 5. The $\delta^{44/40}Ca$ values of seawater calculated from the $\delta^{44/40}Ca$ records of *G. trilobus* (diamonds) and *G. bulloides* (squares), compared to the record of *De La Rocha and DePaolo* [2000] (circles), renormalized to SRM 915a.
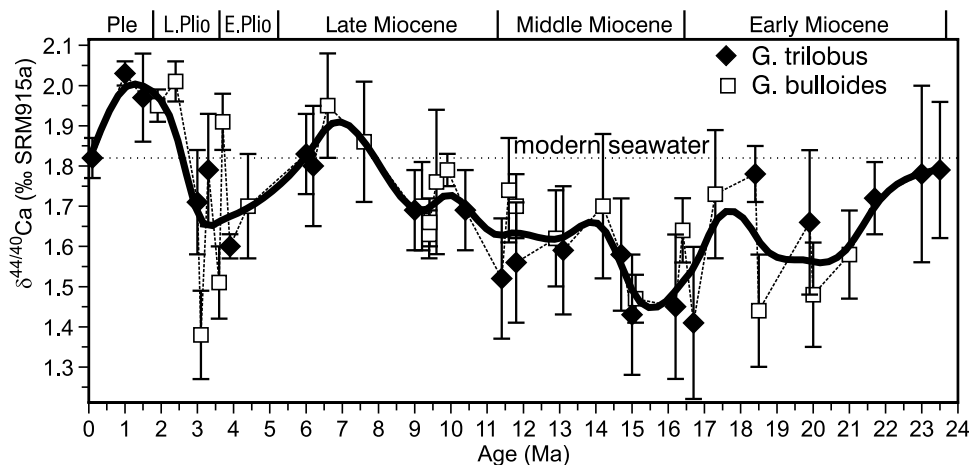
Figure 6. Spline smoothed seawater $\delta^{44/40}$Ca curve for the Neogene, calculated from the stacked $\delta^{44/40}$Ca records of *G. trilobus* and *G. bulloides*. Abbreviations are Ple, Pleistocene; L. Plio, late Pliocene; and E. Plio, early Pliocene. Error bars are $\pm 2\sigma_{mean}$.

seawater and carbonate is diminished at elevated temperatures [*Nägler et al.*, 2000; *Gussone et al.*, 2003]. However, this temperature effect is small in most biogenic and in inorganic carbonate precipitates and has thus no significant effect on the isotopic evolution of seawater. The homogenous isotopic signature of major Ca reservoirs and fluxes implies that changes in the isotopic composition of seawater are probably not caused by variations in the $\delta^{44/40}$Ca values of input and output fluxes [*Schmitt et al.*, 2003b].

[30] Seawater is enriched in ^{44}Ca ($\delta^{44/40}$Ca$_{sw}$ = 1.88‰ [*Schmitt et al.*, 2001; *Hippler et al.*, 2003]) compared to river water and hydrothermal solutions while carbonate sediments, which act as major sink of seawater Ca, are depleted in ^{44}Ca. As a consequence, seawater $\delta^{44/40}$Ca values decrease when riverine and hydrothermal inputs are larger than the removal flux via carbonate formation. Changes in the isotopic composition of seawater may thus reflect changes in the input/output ratio and thereby in the concentration of Ca in seawater [*De La Rocha and DePaolo*, 2000].

[31] Brine inclusion data clearly show that Ca concentrations in seawater have changed considerably over the Phanerozoic [*Horita et al.*, 2002]. It is generally assumed that these changes are caused by secular trends in seafloor spreading and hydrothermal Ca release as imaged by eustatic sea level change [*Hardie*, 1996]. However, recent data imply that spreading rates did not change over the Cenozoic so that coeval changes in seawater Ca have been caused by other alternative processes [*Rowley*, 2002]. Alternative explanations have focused either on sedimentary or on weathering processes. In particular, *Holland and Zimmermann* [2000] proposed that variable rates of dolomite formation may be responsible for the Phanerozoic Ca trends, while *Wallmann* [2001] demonstrated that seawater Ca concentrations may also be affected by changes in the Ca/HCO$_3$ ratio of river water.

6.2. Numerical Calcium/Carbon Cycle Model Approach

[32] We expanded an existing model of the global carbon and calcium cycles [*Wallmann*, 2001] to simulate the

evolution of marine $\delta^{44/40}$Ca$_{sw}$ values. The model considers riverine inputs of Ca originating from carbonate and silicate weathering, hydrothermal inputs, CaCO$_3$ sedimentation, CaCO$_3$ formation during the alteration of oceanic crust and dolomite formation. An isotopic signature is assigned to each of these fluxes (see auxiliary material). Two different scenarios were explored with the model. In the first scenario, we assume that the observed change in the isotopic composition of marine carbonates and seawater has been caused by changes in the riverine Ca flux. Thus the riverine Ca flux is varied so that the resulting marine $\delta^{44/40}$Ca values are consistent with the data. In the second scenario, dolomitization of marine carbonates is considered and assumed to be responsible for the observed $\delta^{44/40}$Ca trends. Hence dolomitization rates are varied to force the model curve through the $\delta^{44/40}$Ca data while riverine Ca fluxes are constrained by the rates of silicate and carbonate weathering calculated in the carbon model.

[33] Figure 7 shows the results of the modeling exercise. It is clearly seen that the $\delta^{44/40}$Ca trends are reproduced by the model only if Ca concentrations in seawater are allowed to change substantially (Figure 7a). The partial pressure of CO$_2$ in the atmosphere (pCO$_2$) decreases over the model period (Figure 7d) because of the continuous increase in physical erosion and chemical weathering [*Wallmann*, 2001]. Total dissolved inorganic carbon follows the same trend (Figure 7c) while the accumulation rate of carbonates at the seafloor (sum of pelagic and platform carbonates, Figure 7g) increases as previously observed [*François and Goddéris*, 1998; *Opdyke and Wilkinson*, 1988].

6.2.1. Variations in the Riverine Ca Flux and Ca/HCO$_3$ Ratios

[34] In the first scenario, the riverine Ca flux and, more significantly, the concentration ratio of Ca to bicarbonate in river water change considerably (Figures 7e and 7f). The riverine Ca/HCO$_3$ ratio reaches a maximum of about 0.5 at the end of the early Miocene. In modern rivers, the Ca/HCO$_3$ ratio is variable pending on the lithology of the drainage area [*Gaillardet et al.*, 1999]. Rivers dominated by the chemical weathering of silicates have molar Ca/HCO$_3$
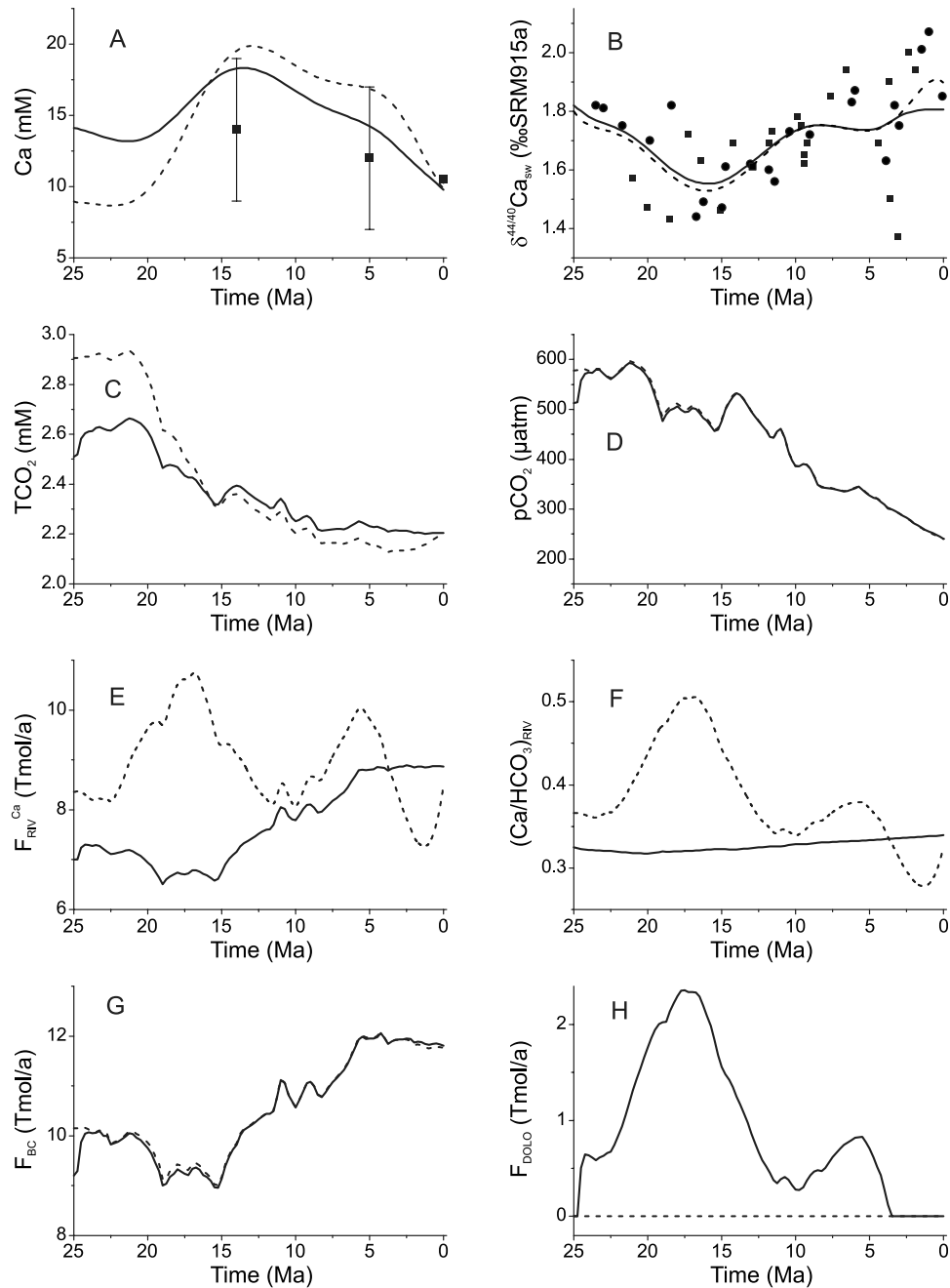
Figure 7. Model results. Dashed lines show the results of a simulation with variable riverine Ca fluxes (scenario 1); solid lines indicate the results of a model run with variable rates of dolomitization (scenario 2). (a) Ca concentrations in seawater. Squares indicate the recent value and the Miocene value derived from brine inclusion data [*Horita et al.*, 2002]. (b) Comparison of the modeled $\delta^{44/40}$Ca variations of seawater and the measured $\delta^{44/40}$Ca variations of *G. bulloides* (squares) and *G. trilobus* (circles). (c) Concentration of total dissolved inorganic carbon in seawater. (d) Partial pressure of CO_2 in the atmosphere. (e) Input of riverine Ca into the oceans. (f) Molar ratio of Ca to HCO_3 in river water. (g) Burial flux of $CaCO_3$ at the seafloor. (h) Rate of Ca release via dolomitization of marine $CaCO_3$.

ratios close to 0.2 while the ratio is about 0.4 in river water affected by carbonate weathering. Evaporite weathering (gypsum and anhydrite) and the release of SO_2 and sulfuric acid in volcanically active terrains may result in riverine Ca/HCO_3 ratios larger than unity. Integrated over entire continents, modern ratios are rather homogenous ranging from

0.21 for Africa to 0.38 for Europe [*Berner and Berner*, 1996]. In the case of our data, weathering would have to be limited almost exclusively to carbonate terrains, evaporite deposits, and volcanic drainage areas to produce a Ca/HCO_3 ratio of 0.5 during the early/middle Miocene. This is an assumption which is not consistent with reconstructions of
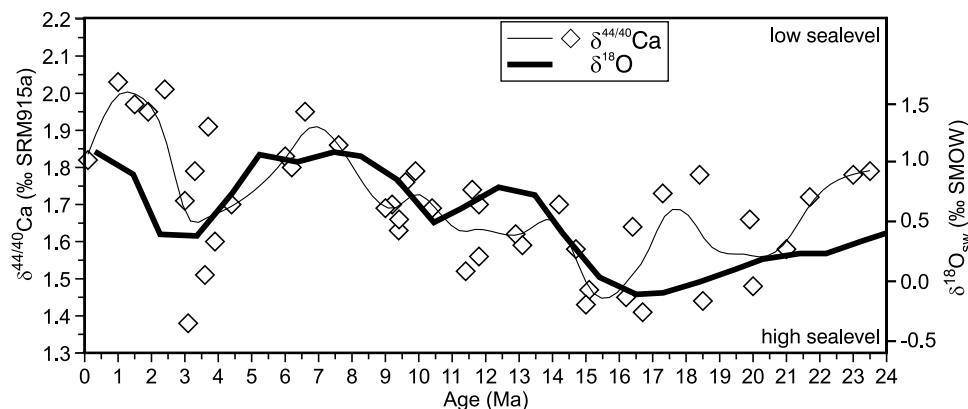
Figure 8. Comparison of the *trilobus/bulloides* $\delta^{44/40}Ca_{sw}$ record and seawater $\delta^{18}O$ as a proxy for sea level, reconstructed from Mg/Ca and $\delta^{18}O$ of benthic foraminifera [*Billups and Schrag*, 2003]. High $\delta^{18}O$ values correspond to low sea level.

rock types exposed during this time, when sea level was high (Figure 8) and erosion of carbonate platforms was limited [*Gibbs et al.*, 1999]. However, the maximum in riverine Ca/HCO₃ ratio coincides with the emplacement of the Columbia flood basalts which was probably accompanied by the massive release of volcanic sulfur gases [*Hansen and Wallmann*, 2003]. Volcanic sulfur gases are oxidized by atmospheric oxygen and the resulting sulfuric acid replaces CO_2 as major weathering agent in volcanic terrains [*Berner and Berner*, 1996]. Hence the Ca/HCO₃ ratio of early/middle Miocene river water might have been enhanced by the massive release of volcanic sulfur gases. On the other hand, the sulfur isotopic record of Cenozoic seawater does not show a significant volcanic signal for the early/middle Miocene [*Paytan et al.*, 1998] suggesting that the volcanic SO_2 release was only of regional rather than of global importance. This lets us conclude that the trends observed in the marine $\delta^{44/40}Ca$ values have very likely not been caused exclusively by changes in the riverine Ca/HCO₃ flux ratio.

6.2.2. Dolomitization

[35] In the second scenario, we model our Ca isotope record by the release of more than 2 Tmol Ca yr^{-1} into the ocean during the early/middle Miocene via dolomitization of marine carbonates. Calcium is released during the process of dolomitization by diffusional exchange with Mg in the reaction

$$2CaCO_3 + Mg^{2+} = MgCa(CO_3)_2 + Ca^{2+}, \qquad (2)$$

eventually increasing the seawater Ca concentration. The released Ca will likely be depleted in ^{44}Ca because of kinetic isotope fractionation [*Artemov et al.*, 1967]. Thus the Ca flux from dolomitization has a relatively low $^{44}Ca/^{40}Ca$ ratio.

[36] Under modern surface conditions, dolomite is only formed during seawater evaporation and in anoxic sedimentary environments [*Morse*, 2003]. However, in the geological past, dolomite formation rates were significantly higher than today, because of a more suitable seawater composition [*Hardie*, 1996; *Stanley and Hardie*, 1998], elevated surface

temperatures [*Arvidson and Mackenzie*, 1999], and extensive seawater evaporation in large-scale marginal basins [*Sun*, 1994]. During the Cenozoic, platform carbonates had rather high dolomite contents while pelagic carbonates were almost exclusively composed of calcite [*Holland and Zimmermann*, 2000]. Dolomite formation may have been rather extensive during the Miocene. For example, dolomite is a major component of the Miocene carbonates of the Florida-Bahamas Platform Complex (>50 vol % in some intervals) and of carbonate platforms deposited in the Mediterranean, Gulf of Suez, and Red Sea [*Holland and Zimmermann*, 2000; *Sun and Esteban*, 1994]. The early/middle Miocene (about 20 to 15 Ma, Burdigalian-Langhian) may have offered exceptionally good environmental conditions for dolomite accumulation. Reefs reached a maximum in latitudinal distribution and the highest abundance of the Cretaceous-Cenozoic [*Kiessling*, 2002]. Carbonate platforms were flooded and expanded by the rising sea level (Figure 8) while surface temperatures increased, further favoring dolomite formation. Moreover, the extensive accumulation of sedimentary organic matter, documented in the marine $\delta^{13}C$ record [*Zachos et al.*, 2001], provided anoxic sedimentary environments where microorganisms may induce rapid and large-scale dolomite formation [*Warthmann et al.*, 2001].

[37] A slightly different situation may have existed for the second proposed dolomitization interval at the end of the Miocene (about 7 to 5 Ma, Messinian). Sedimentation rates of organic carbon again were elevated during this interval, which is known as the "biogenic bloom" [*Diester-Haass et al.*, 2004]. Sea level, however, had dropped significantly since the early Miocene, but was relatively stable during this time (Figure 8) [*Billups and Schrag*, 2003]. Dolomitization at the end of the Miocene is known from several carbonate platforms. For example, at the Bahamas platform an approximately 100 m thick interval of pervasively dolomitized reef carbonates occurs in the upper Miocene of the "Unda" drill core [*Eberli et al.*, 2002].

[38] Hence the second scenario of a dolomite-derived Ca flux seems to be more consistent with the geological record than the first scenario of variable riverine input. We therefore suggest that secular trends in seawater $\delta^{44/40}Ca$ and Ca

concentration are strongly influenced by variable rates of dolomite formation.

7. Summary and Conclusions

[39] It is well accepted that the calcium budget of the oceans has never been at steady state during the Neogene [*Hardie*, 1996; *Wallmann*, 2001; *De La Rocha and DePaolo*, 2000]. Our reconstruction of the Neogene seawater calcium isotope record, however, indicates that fluctuations in the oceanic Ca concentration may have been much more drastic than previously thought. This would have implications for the application of proxies based on element/calcium ratios (e.g., Sr/Ca, Mg/Ca) that rely on relatively stable Ca concentrations in seawater.

[40] The calcium/carbon cycle model simulations show that a significant part of the observed variations in seawater $\delta^{44/40}$Ca can be explained by changes in the Ca input fluxes if the Ca flux was decoupled from the carbonate flux. This decoupling, i.e., a variation of the Ca flux without proportional changes in the HCO_3 flux, is necessary to generate fluctuations in the marine Ca concentration. Otherwise Ca flux variations are compensated by $CaCO_3$ dissolution/precipitation in the oceans.

[41] The coincidence of the most pronounced minimum in our $\delta^{44/40}$Ca record (about 16 Ma) with a period of warm climate and high sea level favors the scenario of increased Ca input from dolomitization. The scenario of an increased Ca/HCO_3 ratio in the riverine input would afford a low sea level with widespread erosion of carbonate sediments from shelves and platforms. However, silicate weathering by sulfuric acid instead of carbonic acid during eruption of the Columbia River flood basalts could have increased the Ca/HCO_3 ratio of the weathering flux and contributed to the observed isotope shift.

[42] The two scenarios are not exclusive and both mechanisms may have contributed to the observed $\delta^{44/40}$Ca variations at varying magnitudes in the course of the Neogene. With that, our $\delta^{44/40}Ca_{sw}$ records clearly indicate that the Neogene calcium cycle was highly dynamic and variable on million year timescales.

References

Antretter, M., B. Steinberger, F. Heider, and H. Soffel (2002), Paleolatitudes of the Kerguelen hotspot: New paleomagnetic results and dynamic modeling, *Earth Planet. Sci. Lett.*, *203*, 635–650.

Antretter, M., H. Inokuchi, and X. Zhao (2003), Paleomagnetic and rock magnetic properties of sediment samples from Ocean Drilling Program leg 183, Kerguelen Plateau, holes 1138A and 1140A [online], *Proc. Ocean Drill. Program Sci. Res.*, *183*. (Available at http://www-odp.tamu.edu/publications/183_SR/004/004_.htm)

Artemov, Y. M., V. P. Strizhov, V. I. Ustinov, and A. A. Yaroshevskiy (1967), Possible isotope fractionation during dolomitization (in Russian), *Geokhimiya*, *5*, 519–529.

Arvidson, R. S., and F. T. Mackenzie (1999), The dolomite problem: Control of precipitation kinetics by temperature and saturation state, *Am. J. Sci.*, *299*, 257–288.

Berner, E. K., and R. A. Berner (1996), *Global Environment: Water, Air, and Geochemical Cycles*, Prentice-Hall, Upper Saddle River, N. J.

Billups, K., and D. P. Schrag (2003), Application of benthic foraminiferal Mg/Ca ratios to questions of Cenozoic climate change, *Earth Planet. Sci. Lett.*, *209*, 181–195.

Birck, J. (1986), Precision K-Rb-Sr isotopic analysis: Application to Rb-Sr chronology, *Chem. Geol.*, *56*, 73–83.

Bohaty, S. M., S. W. Wise, R. A. Duncan, L. C. Moore, and P. J. Wallace (2003), Neogene diatom biostratigraphy, tephra stratigraphy, and chronology of ODP Hole 1138A, Kerguelen Plateau [online], *Proc. Ocean Drill. Program, Sci. Res.*, *183*. (Available at http://www-odp.tamu.edu/publications/183_SR/016/016_.htm)

Böhm, F., A. Eisenhauer, N. Gussone, A. Heuser, A. Haase-Schramm, M. Dietzel, J. Reitner, and J. Vacelet (2002), Fractionation of ^{44}Ca/^{40}Ca between aragonite and calcite, *Geochim. Cosmochim. Acta*, *66*, suppl. 1, A87.

Böhm, F., N. Gussone, A. Eisenhauer, A. Heuser, A. Haase-Schramm, J. Vacelet, J. Reitner, and W.-C. Dullo (2003), Calcium isotopic composition of marine biogenic carbonates: Influences of mineralogy and biology, *Geophys. Res. Abstr.*, *5*, 12,938.

Coffin, M. F., et al. (2000), *Proc. Ocean Drill. Program Initial Rep.* [CD-ROM], *183*, Ocean Drill. Program, College Station, Tex.

Compston, W., and V. Oversby (1969), Lead isotopic analysis using a double spike, *J. Geophys. Res.*, *74*, 4338–4348.

Coplen, T. B., et al. (2002), Compilation of minimum and maximum isotope ratios of selected elements in naturally occurring terrestrial materials and reagents, *U.S. Geol. Surv. Water Resour. Invest. Rep.*, *98*, 98 pp.

De La Rocha, C. L., and D. J. DePaolo (2000), Isotopic evidence for variations in the marine calcium cycle over the Cenozoic, *Science*, *289*, 1176–1178.

Diester-Haass, L., P. A. Meyers, and T. Bickert (2004), Carbonate crash and biogenic bloom in the late Miocene: Evidence from ODP Sites 1085, 1086, and 1087 in the Cape Basin, southeast Atlantic Ocean, *Paleoceanography*, *19*, PA1007, doi:10.1029/2003PA000933.

Eberli, G. P., F. S. Anselmetti, D. Kroon, T. Sato, and J. D. Wright (2002), The chronostratigraphic significance of seismic reflections along the Bahamas Transect, *Mar. Geol.*, *185*, 1–17.

Eisenhauer, A., T. Nägler, P. Stille, J. Kramers, N. Gussone, B. Bock, J. Fietzke, D. Hippler, and A.-D. Schmitt (2004), Proposal for inter-

national agreement on Ca notation resulting from discussion at workshops on stable isotope measurements held in Davos (Goldschmidt 2002) and Nice (EGS-AGU-EUG 2003), *Geostand. Newsl.*, *28*, 149–151.

Farrell, J., and W. Prell (1991), Pacific $CaCO_3$ and δ^{18}O since 4 Ma, paleoceanic and paleoclimatic implications, *Paleoceanography*, *6*, 485–498.

Fietzke, J., A. Eisenhauer, N. Gussone, B. Bock, V. Liebetrau, T. F. Nägler, H. J. Spero, J. Bijma, and C. Dullo (2004), Direct measurement of ^{44}Ca/^{40}Ca ratios by MC-ICP-MS using the cool-plasma-technique, *Chem. Geol.*, *206*, 11–20.

Flower, B. P., and J. P. Kennett (1994), The middle Miocene climatic transition: East Antarctic ice sheet development, deep ocean circulation and global carbon cycling, *Palaeogeogr. Palaeoclimatol. Palaeoecol.*, *108*, 537–555.

François, L. M., and Y. Goddéris (1998), Isotopic constraints on the Cenozoic evolution of the carbon cycle, *Chem. Geol.*, *145*, 177–212.

Frey, F. A., M. F. Coffin, P. J. Wallace, and D. Weis (2003), Leg 183 synthesis: Kerguelen Plateau-Broken Ridge—A large igneous province [online], *Proc. Ocean Drill. Program Sci. Results*, *183*. (Available at http://www-odp.tamu.edu/publications/183_SR/183sr.htm)

Gaillardet, J., B. Dupré, P. Louvat, and C. J. Allègre (1999), Global silicate weathering and CO_2 consumption rates deduced from the chemistry of large rivers, *Chem. Geol.*, *159*, 3–30.

Gibbs, M. T., G. J. S. Bluth, P. J. Fawcett, and L. R. Kump (1999), Global chemical erosion over the last 250 My: Variations due to

changes in paleogeography, paleoclimate, and paleogeology, *Am. J. Sci.*, *299*, 611–651.

Gussone, N., A. Eisenhauer, A. Heuser, M. Dietzel, B. Bock, F. Böhm, H. J. Spero, D. W. Lea, J. Bijma, and T. F. Nägler (2003), Model for kinetic effects on calcium isotope fractionation (δ^{44}Ca) in inorganic aragonite and cultured planktonic foraminifera, *Geochim. Cosmochim. Acta*, *67*, 1375–1382.

Gussone, N., A. Eisenhauer, R. Tiedemann, G. H. Haug, A. Heuser, B. Bock, T. F. Nägler, and A. Müller (2004), Reconstruction of Caribbean sea surface temperature and salinity fluctuations in response to the Pliocene closure of the Central American gateway and radiative forcing, using $\delta^{44/40}$Ca, δ^{18}O and Mg/Ca ratios, *Earth Planet. Sci. Lett.*, *227*, 201–214.

Haggerty, J. A., I. Premoli Silva, F. Rack, and M. K. McNutt (Eds.) (1995), *Proceedings of Ocean Drilling Program, Scientific Results*, vol. 144, Ocean Drill. Program, College Station, Tex.

Hansen, K. W., and K. Wallmann (2003), Cretaceous and Cenozoic evolution of seawater composition, atmospheric O_2 and CO_2: A model perspective, *Am. J. Sci.*, *303*, 94–148.

Hardie, L. A. (1996), Secular variation in seawater chemistry: An explanation for the coupled secular variation in the mineralogies of marine limestones and potash evaporites over the past 600 m. y., *Geology*, *24*, 279–283.

Harris, N. (1995), Significance of weathering Himalayan metasedimentary rocks and leucogranites for the Sr isotope evolution of seawater during the early Miocene, *Geology*, *23*, 795–798.

Hastings, D. W., A. D. Russell, and S. R. Emerson (1998), Foraminiferal magnesium in *G. sacculifer* as paleotemperature proxy, *Paleoceanography*, *13*, 161–169.

Hemleben, C., M. Spindler, and O. R. Anderson (1989), *Modern Planktonic Foraminifera*, Springer, New York.

Heuser, A., A. Eisenhauer, N. Gussone, B. Bock, B. T. Hansen, and T. F. Nägler (2002), Measurement of calcium isotopes (δ^{44}Ca) using a multicollector TIMS technique, *Int. J. Mass. Spectrom.*, *220*, 387–399.

Hippler, D., N. Gussone, K. Darling, A. Eisenhauer, and T. F. Nägler (2002), δ^{44}Ca in *N. pachy* (left): A new SST-proxy in polar regions, *Geochim. Cosmochim. Acta*, *66*, suppl. 1, A331.

Hippler, D., A.-D. Schmitt, N. Gussone, A. Heuser, P. Stille, A. Eisenhauer, and T. F. Nägler (2003), Calcium isotopic composition of various reference materials and seawater, *Geostand. Newsl.*, *27*, 13–19.

Holland, H. H., and H. Zimmermann (2000), The dolomite problem revisited, *Int. Geol. Rev.*, *42*, 481–490.

Horita, J., H. Zimmermann, and H. D. Holland (2002), Chemical evolution of seawater during the Phanerozoic: Implications from the record of marine evaporites, *Geochim. Cosmochim. Acta*, *66*, 3733–3756.

Jacobson, A. D., J. D. Blum, C. P. Chamberlain, M. A. Poage, and V. F. Sloan (2002), Ca/Sr and Sr isotope systematics of a Himalayan glacial chronosequence: Carbonate versus silicate weathering rates as a function of landscape surface age, *Geochim. Cosmochim. Acta*, *66*, 13–27.

Kennett, J. P., and M. S. Srinivasan (1983), *Neogene Planktonic Foraminifera*, John Wiley, Hoboken, N. J.

Kiessling, W. (2002), Secular variations in the Phanerozoic reef ecosystem, *SEPM Spec. Publ. Soc. Sediment. Geol.*, *72*, 625–690.

Lea, D. W., D. K. Pak, and H. J. Spero (2000), Climate impact of late Quaternary equatorial Pacific Sea surface temperature variations, *Science*, *289*, 1719–1724.

Lear, C. H., H. Elderfield, and P. A. Wilson (2000), Cenozoic deep-sea temperatures and global ice volumes from Mg/Ca in benthic foraminiferal calcite, *Science*, *287*, 269–272.

Lemarchand, D., G. J. Wasserburg, and D. A. Papanastassiou (2004), Rate-controlled calcium isotope fractionation in synthetic calcite, *Geochim. Cosmochim. Acta*, *68*, 4665–4678.

Levitus, S., and T. Boyer (1994), *World Ocean Atlas 1994*, vol. 4, *Temperature*, NOAA Atlas NESDIS 4, 129 pp., Natl. Oceanic and Atmos. Admin., Silver Spring, Md.

Lyle, M. (2003), Neogene carbonate burial in the Pacific Ocean, *Paleoceanography*, *18*(3), 1059, doi:10.1029/2002PA000777.

Marriott, C. S., G. M. Henderson, N. S. Belshaw, and A. W. Tudhope (2004), Temperature dependence of δ^7Li, δ^{44}Ca and Li/Ca during growth of calcium carbonate, *Earth Planet. Sci. Lett.*, *222*, 615–624.

Morse, J. W. (2003), Formation and diagenesis of carbonate sediments, in *Treatise on Geochemistry*, vol. 7, edited by F. T. Mackenzie, pp. 67–85, Elsevier, New York.

Nägler, T. F., A. Eisenhauer, A. Müller, C. Hemleben, and J. Kramers (2000), The δ^{44}Ca-temperature calibration on fossil and cultured Globigerinoides sacculifer: New tool for reconstruction of past sea surface temperatures, *Geochem. Geophys. Geosyst.*, *1*, doi:10.1029/2000GC000091.

Opdyke, B. N., and B. H. Wilkinson (1988), Surface area control of shallow cratonic to deep marine carbonate accumulation, *Paleoceanography*, *3*, 685–703.

Paytan, A., M. Kastner, D. Campbell, and M. H. Thiemens (1998), Sulfur isotopic composition of Cenozoic seawater sulfate, *Science*, *282*, 1459–1462.

Paytan, A., E. J. Morris, and R. C. Thunnell (2004), Ca isotopes in foraminifera from sediment traps in the Guyama Basin, paper presented at 8th International Conference on Paleoceanography, Environ. Paleoenviron. Ocean., Biarritz, France.

Pearson, P. N. (1995), Planktonic foraminifer biostratigraphy and the development of pelagic caps on guyots in the Marshall Island group, *Proc. Ocean Drill. Program Sci. Results*, *144*, 21–59.

Pearson, P. N., and M. R. Palmer (2000), Atmospheric carbon dioxide concentrations over the past 60 million years, *Nature*, *406*, 695–699.

Pearson, P. N., and N. J. Shackleton (1995), Neogene multispecies planktonic foraminiferal stable isotope record, Site 871, Limalok Guyot, *Proc. Ocean Drill. Program Sci. Res.*, *144*, 401–410.

Pearson, P. N., N. J. Shackleton, and M. A. Hall (1997), Stable isotopic evidence for the sympactric divergence of *Globigerinoides trilobus* and *Orbulina universa* (planktonic foraminifera), *J. Geol. Soc. London*, *154*, 295–302.

Premoli Silva, I., J. A. Haggerty, and F. R. Rack (1993), *Proc. Ocean Drill. Program Initial Rep.* [CD-ROM], *144*, Ocean Drill. Program, College Station, Tex.

Rosenthal, Y., E. A. Boyle, and N. Slowey (1997), Temperature control on the incorporation of magnesium, strontium, fluorine and calcium into benthic foraminiferal shells from

Little Bahama Bank: Prospect for thermocline paleoceanography, *Geochim. Cosmochim. Acta*, *61*, 3633–3643.

Rowley, D. B. (2002), Rate of plate creation and destruction: 180 Ma to present, *GSA Bull.*, *114*, 927–933.

Schmitt, A.-D., G. Bracke, P. Stille, and B. Kiefel (2001), The calcium isotope composition of modern seawater determined by thermal ionisation mass spectrometry, *Geostand. Newslett.*, *25*, 267–275.

Schmitt, A.-D., P. Stille, and T. Vennemann (2003a), Variations of the ^{44}Ca/^{40}Ca ratio in seawater during the past 24 million years: Evidence from δ^{44}Ca and δ^{18}O values of Miocene phosphates, *Geochim. Cosmochim. Acta*, *67*, 2607–2614.

Schmitt, A.-D., F. Chabaux, and P. Stille (2003b), The calcium riverine and hydrothermal isotopic fluxes and the oceanic calcium mass balance, *Earth Planet. Sci. Lett.*, *213*, 503–518.

Shevenell, A. E., J. P. Kennett, and D. W. Lea (2004), Middle Miocene Southern Ocean cooling and Antarctic cryosphere expansion, *Science*, *305*, 1766–1770.

Skulan, J. L., D. J. DePaolo, and T. L. Owens (1997), Biological control of calcium isotopic abundances in the global calcium cycle, *Geochim. Cosmochim. Acta*, *61*, 2505–2510.

Stanley, S. M., and L. A. Hardie (1998), Secular oscillations in the carbonate mineralogy of reef-building and sediment-producing organisms driven by tectonically forced shifts in seawater chemistry, *Palaeogeogr. Palaeoclimatol. Palaeoecol.*, *144*, 3–19.

Soudry, D., I. Segal, Y. Nathan, C. R. Glenn, L. Halicz, Z. Lewy, and D. L. VonderHaar (2004), ^{44}Ca/^{42}Ca and ^{143}Nd/^{144}Nd isotope variations in Cretaceous-Eocene Tethyan francolites and their bearing on phosphogenesis in the southern Tethys, *Geology*, *32*, 389–392.

Sun, S. Q. (1994), A reappraisal of dolomite abundance and occurrence in the Phanerozoic, *J. Sediment. Res., Sect. A*, *64*, 396–404.

Sun, S. Q., and M. Esteban (1994), Paleoclimatic controls on sedimentation, diagenesis, and reservoir quality: Lessons from Miocene carbonates, *AAPG Bull.*, *78*, 519–543.

Vance, D., and K. Burton (1999), Neodymium isotopes in planktonic foraminifera: A record of the response of continental weathering and ocean circulation rates to climate change, *Earth Planet. Sci. Lett.*, *173*, 365–379.

Vigour, R., and D. Lazarus (2002), Biostratigraphy of late Miocene-early Pliocene radiolarians from ODP Leg 183 Site 1138 [online], *Proc. Ocean Drill. Program Sci. Results*, *183*, 183SR-007. (Available at http://www-odp. tamu.edu/publications/183_SR/007/007_.htm)

Wallmann, K. (2001), Controls on the Cretaceous and Cenozoic evolution of seawater composition, atmospheric CO_2 and climate, *Geochim. Cosmochim. Acta*, *65*, 3005–3025.

Warthmann, R., Y. v. Lith, C. Vasconcelos, J. A. McKenzie, and A. M. Karpoff (2001), Bacterially induced dolomite precipitation in anoxic culture experiments, *Geology*, *28*, 1091–1094.

Whitehead, J. M., and A. McMinn (2002), Kerguelen Plateau Quaternary-late Pliocene palaeoenvironments: From diatom, silicoflagellate and sedimentological data, *Palaeogeogr. Palaeoclimatol. Palaeoecol.*, *186*, 335–368.

Zachos, J. C., M. Pagani, L. C. Sloan, E. Thomas, and K. Billups (2001), Trends, rhythms, and aberrations in global climate 65 Ma to present, *Science*, *292*, 686–693.

Zhu, P., and J. Macdougall (1998), Calcium isotopes in the marine environment and the

oceanic calcium cycle, *Geochim. Cosmochim. Acta*, *62*, 1691–1698.

———————————

F. Böhm, W.-C. Dullo, A. Eisenhauer, A. Heuser, and K. Wallmann, Leibniz-Institut für Meereswissenschaften, Wischhofstr. 1–3, 24148 Kiel, Germany. (fboehm@ifm-geomar.de)

N. Gussone, Forschungszentrum Ozeanränder, Universität Bremen, Postfach 330440, D-28334 Bremen, Germany.

T. F. Nägler, Institut für Geologie, Gruppe Isotopengeologie, Universität Bern, Erlacherstr. 9a, 3012 Bern, Switzerland.

P. N. Pearson, Department of Earth Sciences, Cardiff University, P.O. Box 914, Main Building, Park Place, Cardiff CF10 3YE, UK.